Towards bulk based preconditioning for quantum dot computations

Jack Dongarra, Julien Langou,
and Stanimire Tomov
Computer Science Department
The University of Tennessee
Knoxville, TN 37996-3450

Andrew Canning, Osni Marques,
Christof Vömel, and Lin-Wang Wang
Computational Research Division
Lawrence Berkeley National Laboratory
Berkeley, CA 94720

Abstract— This article describes how to accelerate the convergence of Preconditioned Conjugate Gradient (PCG) type eigensolvers for the computation of several states around the band gap of colloidal quantum dots. Our new approach uses the Hamiltonian from the bulk materials constituent for the quantum dot to design an efficient preconditioner for the folded spectrum PCG method. The technique described shows promising results when applied to CdSe quantum dot model problems. We show a decrease in the number of iteration steps by at least a factor of 4 compared to the previously used diagonal preconditioner.

I. INTRODUCTION

Current nanotechnology advances allow for the lab synthesis of tiny crystals ranging from a few hundred to a few thousand atoms in size called quantum dots (QDs). The quantum dot's electronic properties strongly depend on their shape and size. Therefore, by designing QDs of proper shape and size one can specifically tune their electronic properties which enables remarkable applications. The mathematical simulation of the physical system serves as an important tool to help the understanding of observed phenomena and can also guide future experimental research. In this respect, the demand to investigate more complex systems of increasingly larger numbers of atoms requires significant methodological improvements to make our current computational algorithms scalable.

The simulation of quantum dots is based on first-principles electronic structure calculations which are typically carried out by minimizing the quantum-mechanical total energy with respect to its electronic and atomic degrees of freedom. Under various assumptions and simplifications [1], [12], the electronic part of this minimization problem becomes equivalent to solving the single particle Schrödinger-type equations

$$\hat{H}\psi_i(r) = \epsilon_i\psi_i(r), \tag{1}$$

$$\hat{H} = -\frac{1}{2}\nabla^2 + V$$

where $\hat{H}$ represents the Hamiltonian of the system, $\psi_i(r)$ denotes the single particle wave function with energy ϵ_i and V is the potential of the system. The wave functions are most commonly expanded in plane-waves (Fourier components) up to some cut-off energy. This results in a discretized version of equation (1).

In the approach used in Parallel Energy SCAN (PESCAN) developed by L-W. Wang and A. Zunger [20], [8], a semi-empirical potential or a charge patching method [19] is used to construct V and only some eigenstates of interest around a given energy level E_{ref} are calculated, allowing the study of large nanosystems (up to a million atoms). In its discretized form, the Hamiltonian matrix is Hermitian with dimension equal to the number of Fourier components used to expand the wave functions. Its eigenvalues are real, and the eigenvectors can be chosen to be orthonormal.

In the context of the Self-Consistent Field iteration [13], [14], a large number of eigenstates of (1) need to be computed, see for example [16]. On the other hand, there are situations where only a *small* number of eigenstates of (1) are relevant. In semiconductor quantum dots, the spectrum of the Hamiltonian has an energy gap. Of particular interest to physicists are a few, say 4 to 10, of the interior eigenvalues on either side of the gap which determine many of the electronic properties of the system. Due to its large size, the Hamiltonian is never explicitly computed. The kinetic energy part is represented in Fourier space where it is diagonal, and the potential energy part is evaluated in real space so that the number of calculations used to construct the matrix-vector product scales as $n \log n$ rather than n^2 where n is the dimension of H. Three-dimensional FFTs are used to move between Fourier and real space. H is therefore available only implicitly, as a procedure for computing the matrix-vector product Hx for a given vector x. This requires a matrix free eigensolver. Finally, repeated eigenvalues (degeneracies) due to physical symmetries are possible in the systems that we consider.

In this paper, we study how to accelerate the Preconditioned Conjugate Gradient (PCG) eigensolver available in the PESCAN package [8]. The PCG method has been proven to be efficient and practical for the physical problems that we are solving [20].

To find interior eigenvalues close to E_{ref} with the PCG algorithm, we use a spectral transformation, the *folded spectrum* method [21]. The interior eigenvalue problem is transformed to find the smallest eigenvalues of

$$(H - E_{ref}I)^2 x = \mu x, \tag{2}$$

see Figure 1, top. A well-known drawback of this approach is

that the transformation in general *clusters* the eigenvalues of interest which decreases the rate of convergence of PCG.

Because of these difficulties, the choice of the right preconditioner for PCG is *crucial* to accelerate the convergence. This is a field of active research, see [9]. Our contribution is the development of a new preconditioner, based on bulk material properties, that improves the convergence of PCG.
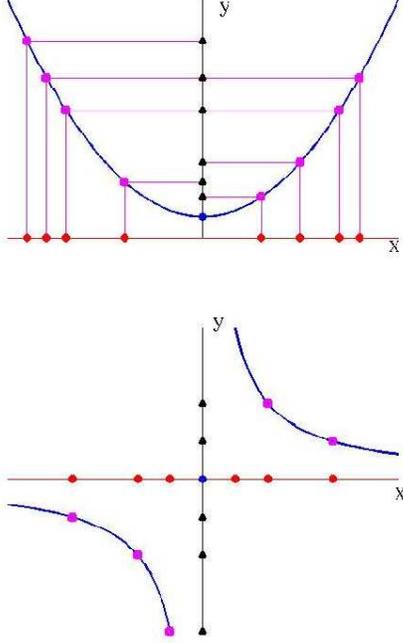
Fig. 1.   Illustration of spectral transformations for the interior eigenvalue problem. Comparison of folded spectrum (top) and shift and invert (bottom). Shown are discrete spectral values of a matrix on the x-axis and the discrete spectrum of the transformed matrix on the y axis. The y-axes intersects x at the point of interest E_{ref}.

The rest of the paper is organized as follows. In Section II we explain the relationship between colloidal quantum dot and bulk band (BB) structure. The Preconditioned Conjugate Gradient (PCG) method is explained in Section III. Next, in Section IV, we show how to use bulk band information in the derivation of BB-type preconditioners for CG. Section V summarizes our computational results. Finally, in Section VI, we give conclusions and some possibilities to further extend this work.

II. QUANTUM DOT AND BULK BAND STRUCTURE

The properties of ideal bulk systems such as crystals are well understood by material scientists. These so-called Bloch states can be computed relatively cheaply because only a few atoms are sufficient to describe the periodic crystal structure.

In contrast, quantum dots represent more complicated physical objects where bulk materials constitute the interior and vacuum the exterior. They can consist of thousands of atoms. However, the key observation on which we base our approach

is that for large enough systems, the converged quantum dot states around the band gap have a small angle to the subspace defined by the corresponding bulk system states. Thus, the information on the properties of a bulk system can be used to guide the computation of a quantum dot consisting of bulk material [22]. This relationship is depicted in Figure 2.
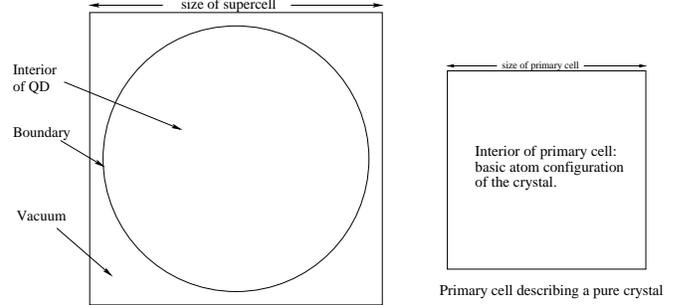
Supercell: quantum dot (QD) in vacuum

Fig. 2.   A supercell with a large quantum dot inside vacuum on the left, a primary cell of a crystal (right).

A. Periodic systems

We describe the structure of the solution of the periodic bulk system as given by Bloch's theorem [7].

1) Bloch's theorem: We consider a system with periodicity A^3. The periodicity of the bulk in terms of this crystal unit corresponds to a periodic potential satisfying

$$V(r + A) = V(r). \tag{3}$$

Bloch's theorem states that the eigenvectors (wave functions) of the Hamiltonian H are of the form

$$\Psi_{nk}(r) = u_{nk}(r)e^{ikr}, \ u_{nk}(r + A) = u_{nk}(r). \tag{4}$$

We denote the corresponding eigenvalues (energies) by E_{nk}.

In the above theorem, k is a priori arbitrary. For any k, eigenpairs $n = 1, 2, \ldots$ can be found. The convention of two indexes n and k is physically motivated.

2) Periodicity of the primary cell and the supercell solution: Let's denote by a the size of the primary cell, and by na the size of the supercell. For any given k, the Fourier expansion of the Bloch solution

$$u_{nk} = \sum_G c_{nG}e^{iGr} \quad \text{yields} \tag{5}$$

$$\Psi_{nk}(r) = \sum_G c_{nG}e^{i(G+k)r}. \tag{6}$$

The admissible Gs are determined by the periodicity requirement for u_{nk}. Namely, only those Fourier components are allowed that have periodicity a, i.e

$$e^{iG(r+a)} = e^{iGr} \ \Leftrightarrow \ G = \frac{2\pi}{a}j, j = 1, 2, \ldots \tag{7}$$

In three dimensions, the set of G vectors becomes the G-grid (lattice) of all these G^3. We call the space

$$\text{span}\{\Psi_{nk}, \ G\text{-admissible}\}$$

the BB space, and denote it by S_{BB}.

The same argument of periodicity applied to the supercell requires that the Fourier expansion of the supercell solution is of the form

$$\Psi(r) = \sum_q c_q e^{iqr}, \quad \text{where} \tag{8}$$

$$e^{iq(r+na)} = e^{iqr} \ \Leftrightarrow \ q = \frac{2\pi}{na}j, j = 1, 2, \ldots. \tag{9}$$

Similarly to the G-grid, the set of admissible q-vectors is called q-grid. We denote the space

$$\text{span}\{\Psi, \ q\text{-admissible}\}$$

by S.

B. Bloch solutions on the q-grid and energy cutoff

The BB-based preconditioners involves transfers ('prolongations'/restrictions) between the G and q-grids. To make these operations efficient we require that $S_{BB} \subset S$, i.e. the G-grid needs to 'fit' onto the q-grid. For this, we choose k to satisfy

$$G + k = q. \tag{10}$$

For complexity reasons, the expansion (8) is truncated. Only the components inside the E_{cut} sphere (the set of q-s such that $|q| < E_{cut}$) are taken into account, a saving of a factor of about 8.

$$\Psi(r) = \sum_{q, |q| < E_{cut}} c_q e^{iqr}. \tag{11}$$

For the Bloch solution (6), a restriction to the same E_{cut} sphere using (10) yields

$$\Psi_{nk}(r) = \sum_{G, |G| < E_{cut}} c_{nG} e^{i(G+k)r}, \tag{12}$$

with the k from the so-called first Brillouin zone.

The relationship between the different grids/Fourier components is depicted on Figure 3.

C. The H_{BB} operator

We define H_{BB} to be the Hamiltonian stemming from the discretization of the Schrödinger's equation for a bulk system. Following the notations in Subsection II-A.2 the eigenfunctions of H_{BB} are $\Psi_{nk}(r)$ with corresponding energies E_{nk}. It follows that for $x(r) \in S_{BB}$, and in particular for

$$x(r) = \sum_{n,k} x_i \Psi_{nk}(r),$$

we have

$$H_{BB} \, x(r) \equiv \sum_{n,k} E_{nk} \, x_i \Psi_{nk}(r). \tag{13}$$
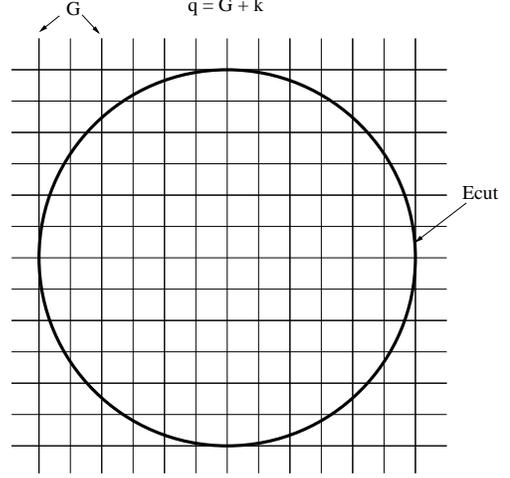
Fig. 3.   The G-grid embedded into the q-grid.

H_{BB}^{-1}, and in particular

$$\tilde{H}_{BB}^{-1} \equiv (H_{BB} - E_{ref}I)^{-2}$$

will be of interest in defining the new preconditioners in Section IV. The product of these operators with $x(r)$ can be expressed correspondingly as

$$H_{BB}^{-1} \, x(r) = \sum_{n,k} E_{nk}^{-1} \, x_i \Psi_{nk}(r) \tag{14}$$

and

$$\tilde{H}_{BB}^{-1} \, x(r) = \sum_{n,k} (E_{nk} - E_{ref})^{-2} \, x_i \Psi_{nk}(r). \tag{15}$$

We first note that the pairs $\Psi_{nk}(r)$, E_{nk} can be easily precomputed. Second, we define the L^2 projection Q^T of functions $R(r) \in S$ to S_{BB} (q-grid to G-grid) by

$$Q^T R(r) = \sum_{n,k} \Psi_{nk}(r) \int u_{nk}(r') e^{-ik \cdot r'} R(r') \, dr' \tag{16}$$

$$\equiv \sum_{n,k} \nu_{nk} \Psi_{nk}(r), \tag{17}$$

and note that this can be efficiently computed in the Fourier space. It follows that quantities like $H_{BB}^{-1} Q^T R(r)$ can be efficiently computed as well.

We denote by Q the prolongation operator from S_{BB} to S. Since $S_{BB} \subset S$ this prolongation operator is the identity. We note that in matrix notations though the prolongation is the transpose of the corresponding restriction matrix.

III. THE PRECONDITIONED CG (PCG) ALGORITHM

The PCG method [20] is the original method used in ESCAN (see the references in [10] and also [12], [3], [2]). It is described in Table I.

The algorithm successively minimizes the Rayleigh quotient function $\rho(x_i) = (x_i^H A x_i)/(x_i^H x_i)$, where the (scaled) gradient is given by $\nabla \rho(x_i) = A x_i - x_i \rho(x_i)$.

```
1      do i = 1,niter
2        do m = 1,numEvals
3          orthonormalize X(m) to X(1:m−1)
4          ax = A X(m)
5          do j = 1,nline
6            λ(m) = X(m) · ax
7            if (||ax − λ(m) X(m)||₂ < tol .or.
                     j == nline) exit
8            rⱼ₊₁ = (I − X(m) X(m)ᴴ) ax
9            β = (rⱼ₊₁·Prⱼ₊₁)/(rⱼ·Prⱼ)
10           dⱼ₊₁ = −P rⱼ₊₁ + β dⱼ
11           dⱼ₊₁ = (I − X(m)X(m)ᴴ)dⱼ₊₁
12           γ = ||dⱼ₊₁||₂⁻¹
13           θ = 0.5 |atan (2 γ dⱼ₊₁·ax)/(λ(m)−γ² dⱼ₊₁·A dⱼ₊₁)|
14           X(m) = cos(θ) X(m) + sin(θ) γ dⱼ₊₁
15           ax = cos(θ) ax + sin(θ) γ A dⱼ₊₁
16         enddo
17       enddo
18       [X, λ] = Rayleigh − Ritz on span{X}
19     enddo
```

TABLE I

THE PRECONDITIONED CONJUGATE GRADIENT (PCG) ALGORITHM FOR FINDING THE *numEvals* SMALLEST EIGENVALUES OF THE OPERATOR A. WHEN COMPUTING THE SMALLEST EIGENVALUES, THE METHOD IS DIRECTLY APPLIED TO H. OTHERWISE, A REPRESENTS THE FOLDED MATRIX $(H − E_{ref}I)^2$ IN THE INTERIOR EIGENVALUE PROBLEM. FOR A DISCUSSION OF PRECONDITIONERS P, SEE SECTION IV.

The smallest eigenvalue λ of the Hermitian matrix $A \equiv (H−E_{ref}I)^2$ (also the eigenvalue of H closest to the reference point E_{ref}) minimizes the Rayleigh Quotient, that is

$$\lambda = \arg \min_{x \neq 0} \rho(x) \equiv \rho(x_i) = (x_i^H A x_i)/(x_i^H x_i). \quad (18)$$

From a current iterate x_j and a descent direction d_j, the method finds the angle

$$\theta_k = \arg \min \rho(x_{j+1}) \equiv \rho(x_j \cos \theta_j + d_j \sin \theta_j). \quad (19)$$

The descent direction is given by $d_j = -\nabla\rho(x_j) + \beta_j d_{j-1}$, see [10]. A preconditioner P can be used to influence the choice of the descent direction via

$$d_j = -P\nabla\rho(x_j) + \beta_j d_{j-1}. \quad (20)$$

We apply the algorithm in a blocked form where the minimization is performed on a set of vectors X_i. After a number of band-by-band iterations, the Rayleigh-Ritz procedure is invoked to compute the best approximations from the subspace, see also [11].

IV. PRECONDITIONERS FOR THE NONLINEAR CG ALGORITHM

We apply the term preconditioning for eigensolvers in the sense suggested by A. Knyazev in [9], [18]. Our preconditioners are designed to approximate H^{-1} in the case of computing the smallest eigenvalues of the discrete Hamiltonian, and to approximate $(H − E_{ref}I)^{-2}$ in the case of solving the folded

spectrum problem (2). The preconditioners, as described below, are applied to the preconditioned CG method, as briefly described in Section III.

A. *The previously used preconditioner*

The preconditioner that was previously used in ESCAN is diagonal. It is applied in the Fourier space as

$$P = D \equiv (I + (-\frac{1}{2}\nabla^2 + V_{avg} - E_{ref})/E_k)^2$$

where $-\frac{1}{2}\nabla^2$ is the Laplacian (diagonal in the Fourier space), E_{ref} is the shift used in the folded spectrum, V_{avg} is the average potential and E_k is the average kinetic energy of a given initial approximation of a wave function ψ_{init}. See [21] for more information.

B. *New BB-type preconditioners*

We defined several preconditioners based on the H_{BB} operator. We define them as the product of an operator/preconditioner P over a current iteration residual R. The most intuitive one is to first decompose R into its S_{BB} and $S_{BB}^{\perp}$ components, i.e. QQ^TR and $R − QQ^TR$, and second precondition the S_{BB} component with H_{BB}^{-1} and the rest with a diagonal preconditioner D^{-1}, i.e.

$$PR \equiv QH_{BB}^{-1}Q^TR + D^{-1}(R − QQ^TR). \quad (21)$$

We note that this preconditioner is not positive definite and that there haven't been any studies (as far as we are aware) in the literature on whether one should use symmetric and positive definite or indefinite preconditioners for hermitian eigenvalue problems.

We use the nesting of our spaces $S_{BB} \subset S$, and follow the ideas from multigrid preconditioners for linear systems (see for example [5], [4]) to define two other preconditioners. Namely, these are an additive and a multiplicative 'pseudo' 2-level preconditioners. We define the additive one as

$$PR \equiv w \, QH_{BB}^{-1}Q^T \, R + D^{-1}R, \quad (22)$$

where w is a scaling parameter taken to be the inverse of the maximum eigenvalue of $QH_{BB}^{-1}Q^T \, H$.

The multiplicative version is defined as

$$r_1 = D^{-1}R \quad (23)$$
$$r_2 = r_1 + w \, QH_{BB}^{-1}Q^T(R − Hr_1) \quad (24)$$
$$PR \equiv r_2 + D^{-1}(R − Hr_2), \quad (25)$$

where w is again (as above)

$$w = \lambda_{max}^{-1}(QH_{BB}^{-1}Q^T \, H).$$

V. NUMERICAL RESULTS

A numerical motivation of why the new preconditioners will efficiently accelerate the computation is given first by the fact that the converged eigenvectors sought lie almost entirely in the S_{BB} space. For the quantum dot simulations considered below for example the angles between the converged solutions and the S_{BB} space are less than 1 degree. Second, testing the

method on bulk problems shows speedups of the computation, compared with just diagonal preconditioning, of close to an order of magnitude in terms of reduced number of iterations. This is our first type of tests in validating the efficiency of the new preconditioners (described in Subsection V-A). The second test-type is on quantum dot simulations, described in Subsection V-B.
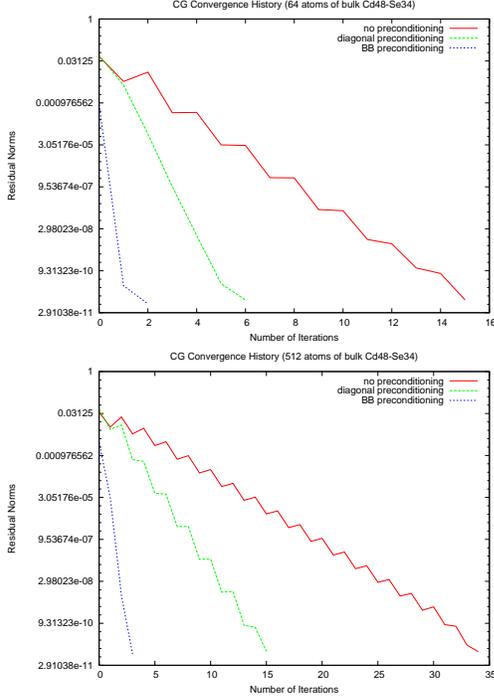
Fig. 4. Convergence histories for test system 1 (top) and 2 (bottom) as described in Subsection V-A.

A. The ground state of a bulk system

This test uses a bulk potential V_{bulk}. We expect the preconditioner to be very effective for ESCAN because if for example we use H_{BB} definition (21), then $H^{-1}v = QH_{BB}^{-1}Q^Tv$ for every $v \in S_{BB}$. In other words, this is the case of an "ideal" preconditioner for the S_{BB} subspace, and therefore also the case when our new preconditioner will be most efficient. Although we can solve this problem in one step by using as an initial guess the bulk solution, in order to numerically demonstrate the efficiency of the method we start with randomly generated initial guess and show the convergence history for bulk problems of increasing size. Finally, before explaining the experiments below, we note that the dimension of the S_{BB} subspace is less then 2% the dimension of the solution space S.

We show results for two test systems. The first consists of 64 atoms of Cd-Se; 32 atoms for each of its 2 components. The second is again for Cd-Se but is of 512 atoms; 256 atoms for each of its components. We use the CG method to compute the 4 lowest eigenstates (15 inner iterations).

The convergence histories for the two test systems are given on Figure 4. We solve for the 4 lowest eigen-states

and the convergence shown is for the 4th. The required accuracy is residual in l^2 norm to be less than 10^{-10}. We get convergence using the new preconditioner in 3 and 4 iterations for correspondingly the first and second test systems. For test system 2 the new method reduces the number of iterations by a factor of 4.

We note that these results do not involve spectral transformation. Applying folded spectrum brings an additional speedup of approximately factor of 2 (see next section) in favor for the new method, and thus making it almost an order of magnitude faster.
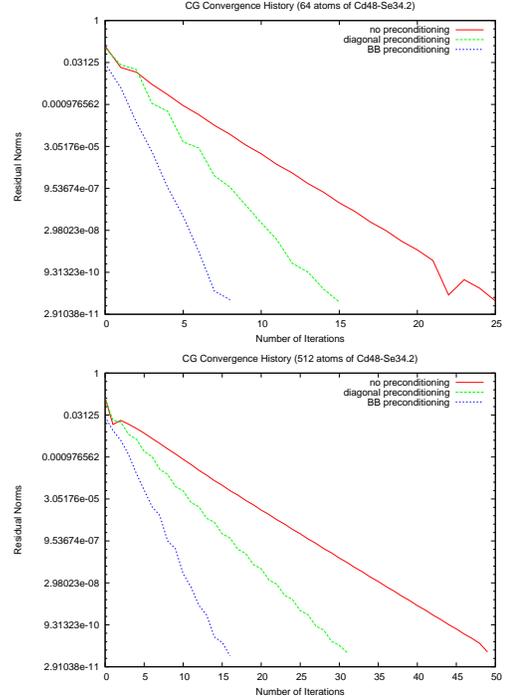
Fig. 5. Convergence histories for test system 1 (top) and 2 (bottom), perturbation for $\gamma = 2$ as described in Subsection V-B.

B. Quantum dot model problems

In this test case we simulate a quantum dot by by adding a second term to the bulk potential, i.e.

$$V = V_{\text{bulk}} + V_{\text{pert}}. \qquad (26)$$

The perturbation term V_{pert} is chosen so that the bulk is confined in the interior of the supercell. Namely, given the center c of the supercell, we choose a radially symmetric function

$$f(r) = ||r - c||^2 - \alpha, \quad \alpha > 0$$

and take

$$V_{\text{pert}}(r) = \max(\gamma f(r), 0),$$

where γ controls the size of the perturbation.

Similarly to the bulk case we consider the 2 test systems from Subsection V-A but with the perturbed potentials as described above. Figure 5 gives convergence histories for

perturbations of *moderate size* ($\gamma = 2$). The graphs on the top are for system 1, and the graphs on the bottom are for system 2. The results show that the new preconditioner reduces the number of iterations (compared to the old preconditioner) by at least a factor of 2.

A bigger test case on a system of $4,096$ atoms is given on Figure 6. Shown is comparison of new (top) *vs* old preconditioner (bottom) for various perturbations.
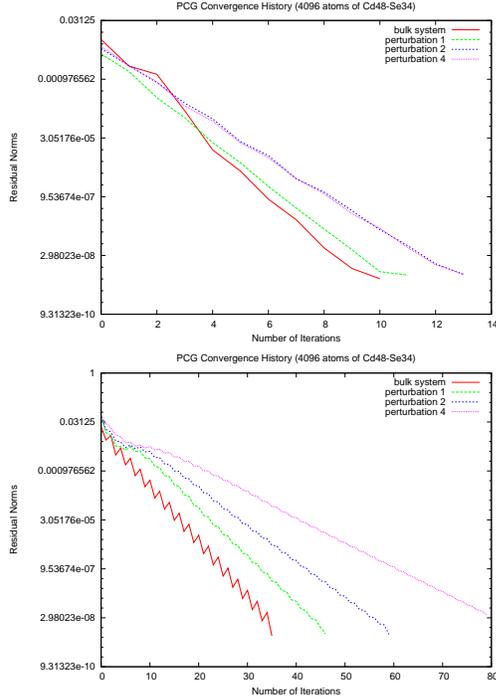
Fig. 6. Convergence histories for test system 3. On the top we show the convergence for various perturbation using the multiplicative version of our preconditioner. On the bottom is the convergence history for using a diagonal preconditioner.

Applying folded spectrum transformation reveals an additional factor of 2 speedup in terms of reduced number of matrix-vector products until desired convergence. A typical result is illustrated for system 2 on Figure 7, where we show a reduced number of iterations by an average factor of 4.

As mentioned in the previous subsection, the dimension of S_{BB} is less then 2% the dimension of the solution space. Still, the angles of the eigenstates sought to the S_{BB} subspace are approximately 0.3, 0.4, and 0.5 for perturbations with γ correspondingly 1, 2, and 4 for test system 2.

VI. CONCLUSIONS AND POSSIBLE EXTENSIONS

In conclusion, we showed a way to use QD bulk properties in accelerating QD computations. The new preconditioner shows promising results in accelerating the computation. It is implemented in the much smaller G-space. Thus there is no need for an FFT, and the nesting of $S_{BB} \subset S$ allows us to efficiently implement H_{BB}^{-1} and the projection operators. The numerical results show the efficiency of the BB-based
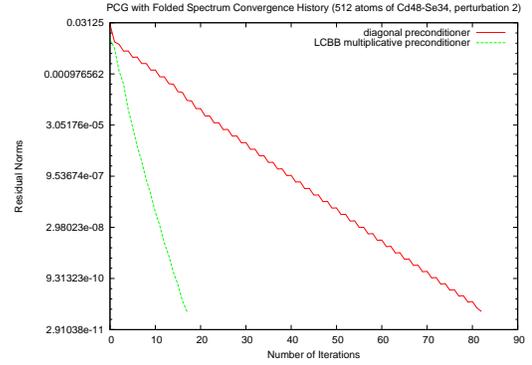
Fig. 7. Comparison of diagonal and BB preconditioning with folded spectrum for test system with perturbation $\gamma = 2$ (right).

computation acceleration as we observe a factor of 4 speedup in terms of reduced number of iterations.

Future work includes testing the new technique on real semi-conductor quantum dots. Other possible extensions of this work include tests on quantum wires.

REFERENCES

[1] Le Bris, C. and Lions, P.-L.: From atoms to crystals: a mathematical journey Bull. Amer. Math. Soc., 42(3), 2005, 291-363.
[2] A. Edelman, T. A. Arias, and S. T. Smith. The geometry of algorithms with orthogonality constraints. *SIAM J. Matrix Anal. Appl.*, 20(2):303–353, 1999.
[3] A. Edelman and S. T. Smith. On conjugate gradient-like methods for eigen-like problems. *BIT*, 36(3):494–508, 1996.
[4] J.H. Bramble, J. E. Pasciak, and J. Xu: Parallel multilevel preconditioners. Math. Comput., 1990, 55, 191, 1-22.
[5] J.H. Bramble and X. Zhang: The Analysis of Multigrid Methods. Handbook of Numerical Analysis, VII (P.G. Ciarlet and J.L. Lions, eds.), North-Holland, Amsterdam, 2000, 173-415.
[6] B. Carpentieri, L. Giraud, and S. Gratton: Additive and multiplicative two-level spectral preconditioning for general linear systems. Technical Report TR/PA/04/38, CERFACS, Toulouse, France, 2004.
[7] N. W. Ashcroft and N. D. Mermin. *Solid state physics*. Saunders College, Philadelphia, 1.st edition, 1976.
[8] A. Canning, L.-W. Wang, A. Williamson and A. Zunger: Parallel Empirical Pseudopotential Electronic Structure Calculations for Million Atom Systems. J. Comp. Phys., 160, 2000, 29-41.
[9] Knyazev, A.: Preconditioned Eigensolvers - an Oxymoron? Electronic Trans. on NA, volume 7, 1998, pp. 104–123
[10] J. Nocedal and S. J. Wright. *Numerical Optimization*. Springer, New York, 1. edition, 1999.
[11] B. N. Parlett. The Symmetric Eigenvalue Problem, SIAM (Classics in Applied Mathematics), Philadelphia, 1998.
[12] Payne, M.C., Teter, M.P., Allan, D.C., Arias, T.A., Joannopoulos, J.D.: Iterative minimization techniques for ab initio total-energy calculations: molecular dynamics and conjugate gradients. Rev. Mod. Phys. **64** (1992) 1045–1097.

[13] P. Pulay. Convergence acceleration of iterative sequences. The case of SCF iteration. *Chem. Phys. Lett.*, 73(2):393–398, 1980.

[14] P. Pulay. Improved SCF Convergence Acceleration. *J. Comp. Chem.*, 3(4):556–560, 1982.

[15] Y. Saad. Numerical Methods for Large Eigenvalue Problems, Manchester University Press, Manchester, England, 1992.

[16] Y. Saad, A. Stathopoulos, J. R. Chelikowsky, K Wu, and S. Ogut. Solution of large eigenvalue problems in electronic structure calculations. *BIT*, 36(3):1–16, 1996.

[17] A. R. Tackett and M. Di Ventra. Targeting Specific Eigenvectors and Eigenvalues of a Given Hamiltonian Using Arbitrary Selection Criteria. *Physical Review B*, 66:245104, 2002.

[18] Z. Bai, J. Demmel, J. Dongarra, A. Ruhe and H. van der Vorst, Eds. Templates for the solution of Algebraic Eigenvalue Problems: A Practical Guide. SIAM, Philadelphia, 2000.

[19] Wang, L.W., Li, J.: First principle thousand atom quantum dot calculations. Phys. Rev. B **69** (2004) 153302

[20] L.-W. Wang and A. Zunger: Solving Schrödinger's equation around a desired energy: application to silicon quantum dots. J. Chem. Phys. **100(3)** (1994) 2394–2397

[21] L.-W. Wang and A. Zunger: *Pseudopotential Theory of Nanometer Silicon Quantum Dots application to silicon quantum dots*. In Kamat, P.V., Meisel, D.(Editors): *Semiconductor Nanoclusters* (1996) 161–207

[22] L.-W. Wang and A. Zunger: Linear combination of bulk band method for strained system million atom nanostructure calculations. Phys. Rev. B 59, 15806, 1999.